Molecules and Cells

Pan-Caspase Inhibitor zVAD Induces Necroptotic and Autophagic Cell Death in TLR3/4-Stimulated Macrophages

Yuan-Shen Chen[1], Wei-Chu Chuang[2], Hsiu-Ni Kung[3], Ching-Yuan Cheng[2], Duen-Yi Huang[2], Ponarulselvam Sekar[4], and Wan-Wan Lin[2,4,5,*]

[1]Department of Neurosurgery, National Taiwan University Hospital Yunlin Branch, Douliu 64041, Taiwan, [2]Department of Pharmacology, College of Medicine, National Taiwan University, Taipei 10617, Taiwan, [3]Graduate Institute of Anatomy and Cell Biology, National Taiwan University, Taipei 10617, Taiwan, [4]Graduate Institute of Medical Sciences, Taipei Medical University, Taipei 11031, Taiwan, [5]Department of Pharmacology, National Defense Medical Center, Taipei 11490, Taiwan
*Correspondence: wwllaura1119@ntu.edu.tw
https://doi.org/10.14348/molcells.2021.0193
www.molcells.org

In addition to inducing apoptosis, caspase inhibition contributes to necroptosis and/or autophagy depending on the cell type and cellular context. In macrophages, necroptosis can be induced by co-treatment with Toll-like receptor (TLR) ligands (lipopolysaccharide [LPS] for TLR4 and polyinosinic-polycytidylic acid [poly I:C] for TLR3) and a cell-permeable pan-caspase inhibitor zVAD. Here, we elucidated the signaling pathways and molecular mechanisms of cell death. We showed that LPS/zVAD- and poly I:C/zVAD-induced cell death in bone marrow-derived macrophages (BMDMs) was inhibited by receptor-interacting protein kinase 1 (RIP1) inhibitor necrostatin-1 and autophagy inhibitor 3-methyladenine. Electron microscopic images displayed autophagosome/autolysosomes, and immunoblotting data revealed increased LC3II expression. Although zVAD did not affect LPS- or poly I:C-induced activation of IKK, JNK, and p38, it enhanced IRF3 and STAT1 activation as well as type I interferon (IFN) expression. In addition, zVAD inhibited ERK and Akt phosphorylation induced by LPS and poly I:C. Of note, zVAD-induced enhancement of the IRF3/IFN/STAT1 axis was abolished by necrostatin-1, while zVAD-induced inhibition of ERK and Akt was not. Our data further support the involvement of autocrine IFNs action in reactive oxygen species (ROS)-dependent necroptosis, LPS/zVAD-elicited ROS production was inhibited by necrostatin-1, neutralizing antibody of IFN receptor (IFNR) and JAK inhibitor AZD1480. Accordingly, both cell death and ROS production induced by TLR ligands plus zVAD were abrogated in STAT1 knockout macrophages. We conclude that enhanced TRIF-RIP1-dependent autocrine action of IFNβ, rather than inhibition of ERK or Akt, is involved in TLRs/zVAD-induced autophagic and necroptotic cell death via the JAK/STAT1/ROS pathway.

Keywords: autophagy, interferon, JAK/STAT1, macrophage, necrosis, zVAD

INTRODUCTION

Cell death is an evolutionarily conserved biological process that is crucial for embryonic development, tissue homeostasis, and immune responses. Several studies have identified various forms of cell death, such as apoptosis, necroptosis, autophagic cell death, and pyroptosis. In addition to the morphological distinction, each type of cell death relies on a subset of proteins and molecular pathways (Denton and Kumar,

Received 23 July, 2021; revised 24 September, 2021; accepted 15 October, 2021; published online 20 December, 2021

eISSN: 0219-1032
©The Korean Society for Molecular and Cellular Biology.
This is an open-access article distributed under the terms of the Creative Commons Attribution-NonCommercial-ShareAlike 3.0 Unported License. To view a copy of this license, visit http://creativecommons.org/licenses/by-nc-sa/3.0/.

2019; Doherty and Baehrecke, 2018; Kist and Vucic, 2021). It is clear that none of these pathways operate alone. Instead, many pathways share components and signaling principles and have intricate connections, even switching the death signals to activate respective death pathways (Kist and Vucic, 2021).

Necroptosis is a recently identified alternative cell death caused by necrosis (Grootjans et al., 2017; Hanson, 2016; Zhang et al., 2020; Zheng and Kanneganti, 2020). This can be induced by caspase inhibition under certain circumstances. Necroptosis is an ancient and evolutionarily conserved cell death modality that participates in several pathogeneses, such as embryonic abortion, ischemic injury, neurodegeneration, viral infection, colitis, and acute kidney injury (Galluzzi et al., 2017; Pasparakis and Vandenabeele, 2015; Xia et al., 2020; Yuan et al., 2019). Recent studies have indicated the involvement of the assembly of a supramolecular complex called the necrosome to mediate the execution of necroptosis. Receptor-interacting protein (RIP) 1 and RIP3 are two Ser/Thr protein kinases that undergo caspase-dependent protein cleavage (Hanson, 2016; Yuan et al., 2019). Inhibition of caspase activity by caspase inhibitors, such as carbobenzoxy-valyl-alanyl-aspartyl-[O-methyl]-fluoromethylketone (zVAD), results in RIP1- and RIP3-contained necrosome formation, and their coordinated kinase activities deliver a pronecrotic signal relying on the production of mitochondrial reactive oxygen species (ROS) (He et al., 2009; Mandal et al., 2020; Vandenabeele et al., 2010a).

Autophagy is an evolutionarily conserved process in innate immunity and metabolism, whereas excess autophagy leads to cell death. Accumulating evidence indicates the interplay between autophagy and necroptosis by observing the co-occurrence of autophagy during the necroptotic process. For example, the RIP1 inhibitor necrostatin-1 (Nec-1) can block light chain 3 (LC3)-II induction and neuronal damage in the retina after ischemia-reperfusion injury (Rosenbaum et al., 2010). Moreover, autophagy-dependent necroptosis has also been demonstrated in palmitic acid-stimulated endothelial cells (Khan et al., 2012) and in ovarian cancer cells with BMI1 inhibition (Dey et al., 2016). Autophagy-dependent necroptosis is an alternative strategy for overcoming the resistance of childhood acute lymphoblastic leukemia (Bonapace et al., 2010).

Toll-like receptors (TLRs) are crucial pattern recognition receptors involved in innate immunity. One mechanism for host defense is the induction of autophagy in macrophages. As reported, TLR4 and TLR3 activation by lipopolysaccharide (LPS) and polyinosinic-polycytidylic acid (poly I:C), respectively, can cause autophagy not only in macrophages via the Toll-IL-1R domain-containing adaptor-inducing IFN-β factor (TRIF)-RIP1 pathway, but also in various cell types, such as cardiomyocytes and cancers (Gao et al., 2018; Lai et al., 2018; Shi and Kehrl, 2008; Xu et al., 2006, 2007). The induction of autophagy by TLR3/4 activation contributes to cancer cell migration and invasion (Zhan et al., 2014) and heart failure after myocardial infarction (Gao et al., 2018). Studies have shown that inhibition of caspase-dependent degradation of TRIF1 and RIP1 by zVAD can induce TRIF/RIP1/ROS-dependent autophagic cell death in TLR3/4 activated macrophages (Jabir et al., 2014; Xu et al., 2006, 2007). In addition to inducing autophagy-dependent cell death, LPS/zVAD and poly I:C/zVAD can induce necroptosis via TRIF/RIP1/RIP3 in macrophages (Seya et al., 2012), cancer cells (Seya et al., 2012; Takemura et al., 2015) and microglia (Kim and Li, 2013). A study further revealed that inhibition or elimination of caspase 8 during stimulation of TLR4 and TLR3 can directly induce TRIF association with the necrosome for cell necroptosis (Kaiser et al., 2013). A recent report further showed that TRIF turnover is regulated by autophagy and downregulation of the autophagy-related gene Atg16l1 promotes TRIF accumulation and its downstream signaling in macrophages (Samie et al., 2018). Although the above studies suggest that the TLR/TRIF signaling axis mediates autophagic and necroptotic death in macrophages under TLR3/4 activation and caspase inhibition, the molecular link between both death modes remains unclear. Therefore, in this study, we used primary BMDMs as the cell model to explore the effects of zVAD on LPS- and poly I:C-induced signaling pathways and the molecular link between autophagy and necroptosis. We found that TRIF-RIP1-dependent autocrine action of interferon-β (IFNβ) may participate in the process of zVAD-induced autophagic and necroptotic death in TLR3- and TLR4-activated macrophages via the JAK/STAT1/ROS pathway.

MATERIALS AND METHODS

Reagents

Dulbecco's modified Eagle's medium (DMEM), fetal bovine serum (FBS), trypsin-ethylenediaminetetraacetic acid (EDTA), penicillin G, and streptomycin were purchased from Invitrogen Corporation (USA). LPS, poly I:C, 3-methyladenine (3-MA), bafilomycin A1, 3-(4,5-cimethylthiazol-2-yl)-2,5-diphenyl tetrazolium bromide (MTT), 2'7'-dichlorodihydrofluorescein diacetate ($DCFH_2$-DA), and butylated hydroxyanisole (BHA) were obtained from Sigma-Aldrich (USA). zVAD was obtained from Bachem (USA). Nec-1, U0126, and PD98059 were obtained from Calbiochem (USA). AZD1480 was purchased from Selleckchem (USA). Mouse type I IFN receptor-neutralizing antibody was purchased from e-Bioscience (USA). The tumor necrosis factor (TNF) receptor neutralizing antibody, Embrel, was purchased from Wyeth (USA). LC3 antibody was purchased from MBL (USA). Antibodies against extracellular signal-regulated kinase (ERK)-2, c-Jun NH2-terminal kinase (JNK)-1, p38, IκB kinase (IKK)-α/β, and signal transducer and activator of transcription protein (STAT)-1, as well as horseradish peroxidase-coupled anti-rabbit and anti-mouse antibodies were purchased from Santa Cruz Biotechnology (USA). Antibodies against phosphorylated IKKα (Ser176)/IKKβ (Ser177), JNK, ERK, p38, Akt, STAT-1, and IRF3 were obtained from Cell Signaling Technology (USA). The antibody against β-actin was obtained from Upstate Biotechnology (USA).

Mice

Wild-type (WT) and $STAT1^{-/-}$ C57BL/6 mice were bred under specific pathogen-free conditions at the Animal Center of the National Taiwan University College of Medicine. The animal experiments were conducted in accordance with institutional

regulations after receiving approval from the Ethics Committee of the National Taiwan University College of Medicine (No. 20130391).

Preparation of BMDMs

Mice at 8-12 weeks of age were killed by cervical dislocation, and both tibias and femurs were dissected free of adherent tissues. The ends of the bones were cut off and flushed by irrigation with DMEM until the bone cavity appeared white. The cells were resuspended by vigorous pipetting and washed by centrifugation at 1,000 rpm for 10 min. The cells were then cultured in 150 mm plastic tissue-culture dishes (Corning, USA) with 25 ml DMEM containing 15% FBS and 20% L929 fibroblast conditional medium as a source of mouse macrophage colony-stimulating factor (M-CSF). The L929 fibroblast conditioned medium was the supernatant of 5×10^5/ml L929 fibroblasts cultured for 7 days in a 75T flask containing 25 ml complete DMEM medium. Macrophages were obtained from adherent cells after 7-10 days of culture. The purity of differentiated macrophages was assessed by staining with antibodies against CD11b-FITC (eBioscience, USA) and F4/80-PE (BD Pharmingen, USA). The cell population of $CD11b^+$ and $F4/80^+$ double-positive cells was 90%, as previously described (Lin et al., 2010). All animals were bred under specific pathogen-free conditions at the Laboratory Animal Center, National Taiwan University College of Medicine (Taiwan). All experimental procedures were approved by the National Taiwan University College of Medicine Ethics Committee in accordance with the guidelines for the care of animals (IACUC No. 20140278).

MTT assay

Cells (10^4/ml) in 96-well plates were incubated with the indicated drugs at 37°C for 24 h. MTT (5 mg/ml) was added for 60 min, the culture medium was removed, and the formazan granules generated by live cells were dissolved in dimethyl sulfoxide (DMSO). The optical density values at 550 nm and 630 nm were measured using a microplate reader. The net absorbance (OD_{550}-OD_{630}) indicates the enzymatic activity of mitochondria and cell viability.

Propidium iodide uptake assay

Cell membrane integrity was assessed by determining the ability of cells to take up propidium iodide (PI). Cells were trypsinized, collected by centrifugation, washed once with phosphate-buffered saline (PBS), and resuspended in PBS containing 25 mg/ml PI. The cells were incubated for 20 min at 37°C. After incubation, the cells were analyzed using FACScan flow cytometry. The level of PI uptake by cells was quantified, and the percentage of cell population with positive PI staining indicating necrosis was determined.

Electron microscopic detection of autophagy

Cells were collected and fixed with 4% paraformaldehyde in 0.1 M cacodylate buffer at 4°C overnight. The cells were then rinsed with cacodylate buffer, post-fixed with 1% osmium tetroxide in 0.1 M cacodylate buffer, dehydrated in a graded series of ethanol (75%, 85%, 95%, and 100%), and embedded in an Epon-araldite mixture. After the resin had solidified, the plastic culture dish was broken up to release the resin containing the embedded cells. Specimens were sectioned with a Diatome diamond knife on a Rechert Ultracut E ultramicrotome (Leica, Germany). Ultrathin sections were stained with uranyl acetate and lead citrate and viewed using an H-7100 electron microscope (Hitachi, Japan). All images were captured using an ORCA-ER CCD digital camera system (Advanced Microscopy Techniques, USA).

Immunoblotting analysis

After the treatment, the medium was aspirated. Cells were rinsed once with ice-cold PBS, harvested, and lysed directly with 1X sodium dodecyl sulfate (SDS) gel-loading buffer (50 mM Tris-HCl, pH 6.8, 2% 2-mercaptoethanol, 0.1% bromophenol blue, and 10% glycerol). Samples were heated at 95°C for 5 min and equal amounts of the whole cell extracts were electrophoresed on 8%-15% SDS-polyacrylamide gel electrophoresis (PAGE), and transferred to Immunobilon-P (Millipore, USA). Membranes were blocked with Tris-buffered saline with Tween 20 (TBST) (50 mM Tris-HCl, pH 7.5, 150 mM NaCl, and 0.1% Tween 20) containing 5% non-fat milk for 1 h at room temperature to minimize nonspecific binding. After hybridization with the primary antibodies, membranes were washed three times with TBST and incubated with a horseradish peroxidase-conjugated secondary antibody for 1 h. After washing three times with TBST, the protein bands were detected using an ECL detection reagent (PerkinElmer [USA] or Millipore). β-Actin was used as the internal control.

Measurement of cytosolic ROS

To measure cytosolic ROS levels, we used $DCFH_2$-DA. After treatment for the indicated time periods, cells were collected and incubated in PBS containing the reagent $DCFH_2$-DA (5 μM) for 30 min at 37°C. After incubation, cells were washed twice with PBS, re-suspended in 0.3 mL PBS, and subjected to flow analysis using a FACScan flow cytometer. The data based on FL1 channels were analyzed using the CellQuest program.

Real-time reverse transcription-polymerase chain reaction with SYBR Green detection

The expression of cytokines and TLR3/4 was determined by real-time reverse transcription-polymerase chain reaction (RT-PCR) analysis. After treatment, the cells were homogenized with 500 μl RNA-Bee isolation reagents (Tel-test), and total RNA was extracted following the commercial standard protocol. Reverse transcription was performed using an RT-PCR kit (Promega, Germany), and 5 μg of total RNA was reverse transcribed to cDNA following commercial standard procedures. The specific primer sequences for IFNβ, IFNα, interleukin (IL)-6, IL-1β, cyclooxygenase (COX)-2, TNF-α, TLR3, and TLR4 were listed in Table 1. Amplification products using SYBR Green detection were routinely checked using dissociation curve software (PerkinElmer Life Science, USA) and by gel electrophoresis on a 1% agarose gel and then visualized under UV light following staining with 0.05% ethidium bromide to confirm the size of the DNA fragment and that only one product was formed. Samples were compared using the relative (comparative) Ct method to analyze the results. The

Table 1. The specific primers for target gene

Gene	Sense	Antisense
TLR3	TCTGGAAACGCGCAAACC	GCCGTTGGACTCTAAATTCAAGAT
TLR4	GCCTTTCAGGGAATTAAGCTCC	AGATCAACCGATGGACGTGTA A
IFNα	TCTGATGCAGCAGGTGGG	AGGGCTCTCCAGAYTTCTGCTCTG
IFNβ	AGCTCCAAGAAAGGACGAACAT	GCCCTGTAGGTGAGGTTGATCT
IL-6	TTCCTCTCTGCAAGAGACTTC	GGTCTGTTGGGAGTGGTATC
IL-1β	TTCAAGGGGACATTAGGCAG	TGTGCTGGTGCTTCATTCAT
TNF-α	ATGAGAAGTTCCCAAATGGCC	TCCACTTGGTGGTTTGCTACG
COX-2	GAGAGAAGGAAATGGCTGCAGAA	GGCTTCCAGTATTGAGGAGAACAGA
Actb	CGGGGACCTGACTGACTACC	AGGAAGGCTGGAAGAGTGC

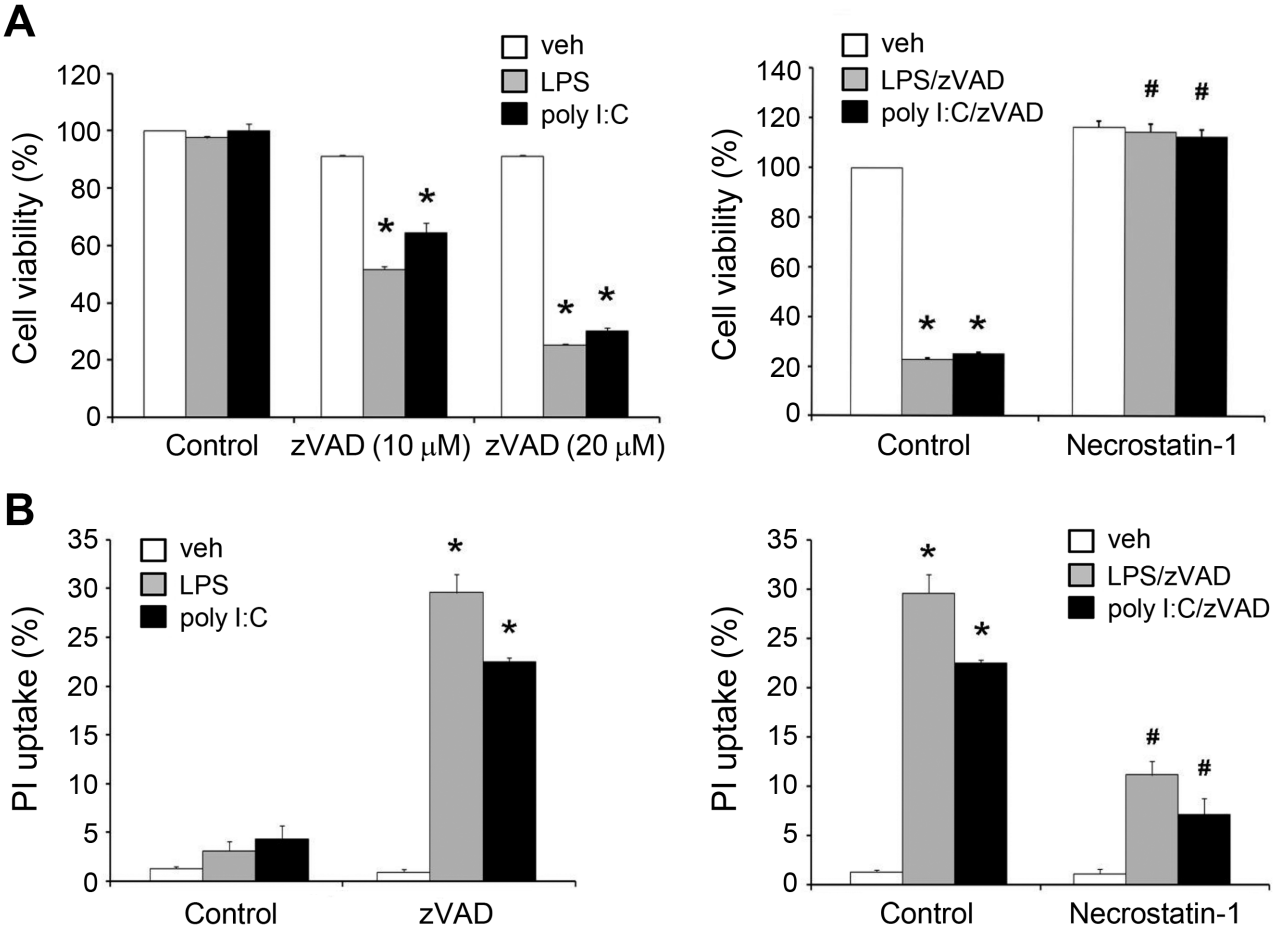

Fig. 1. zVAD co-treatment with TLR3 and TLR4 ligands induces the RIP1-dependent necroptosis in BMDMs. BMDMs were pre-treated with vehicle (veh) or necrostatin-1 (Nec-1) (10 μM) for 30 min, followed by zVAD (20 μM for most experiments or at the indicated concentrations) for another 30 min. Cells were then stimulated with LPS (1 μg/ml) or poly I:C (20 μg/ml) for 24 h, and cell viability was assessed by MTT assay (A) or PI uptake (B). Data were presented as the mean ± SEM from at least three independent experiments. $*P < 0.05$, indicating significant cytotoxic effects. $^{\#}P < 0.05$, indicating a significant effect of Nec-1 in inhibiting cytotoxicity induced by zVAD/TLR ligands.

fold of induction was measured relative to time-matched vehicle-treated controls and calculated after adjusting for β-actin using $2^{-\Delta\Delta Ct}$, where ΔCt = target gene Ct − β-actin Ct, and ΔΔCt = ΔCt treatment − ΔCt control.

Enzyme-linked immunosorbent assay (ELISA)

BMDMs cultured in 3.5 cm dishes were stimulated with the indicated agents at 37°C and 5% CO_2. Culture supernatants were harvested and centrifuged at 1,000 rpm to remove cell debris. The concentration of IFNβ in the supernatants was measured using the DuoSet ELISA development kit (R&D Sys-

tems, USA) according to the manufacturer's instructions.

Phagocytosis

BMDMs (5×10^5) were seeded and stimulated with LPS (1 μg/ml) or poly I:C (20 μg/ml) for 4 h or 8 h at 37°C and 5% CO_2. In the last 1 h, pHrodo *Escherichia coli* bioparticles (Thermo Fischer Scientific, USA) were added at 20 μg/ml. One hour later, the cells were washed and trypsinized, and the phagocytose particles were determined using FACScalibur (BD Biosciences). Mean fluorescence was determined and analyzed using the CellQuest Pro software.

Statistical evaluation

Values were expressed as the mean ± SEM of at least three independent experiments. Student's *t*-test was used to determine the statistical significance ($P < 0.05$).

RESULTS

zVAD induces necroptosis and autophagic cell death in TLR3- and TLR4-activated BMDMs

Before elucidating the molecular events underlying necroptosis upon caspase inhibition, we first treated BMDMs with zVAD and TLR ligands (LPS or poly I:C). LPS (1 μg/ml), poly I:C (20 μg/ml), and zVAD (10 μM or 20 μM) alone failed to change cell viability, whereas co-treatment of zVAD with each TLR ligand for 24 h caused apparent cytotoxicity as assessed by MTT assay (Fig. 1A) or PI uptake (Fig. 1B). Next, we found that LPS/zVAD- and poly I:C/zVAD-induced cell death could be reversed by the necroptosis inhibitor Nec-1 (Fig. 1). We also examined the effects of zVAD on other TLR ligands, including Pam3CysSerLys4 (*Pam*3CSK4) (Pam, TLR2/TLR1 ligand), flagellin (TLR5 ligand), R848 (TLR7/8 ligand), and CpG oligodeoxynucleotides (CpG ODNs) (TLR9 ligand). Nevertheless, we did not observe cell death when these TLR ligands were treated together with zVAD (data not shown), indicating that TRIF- rather than the MyD88-dependent pathway of

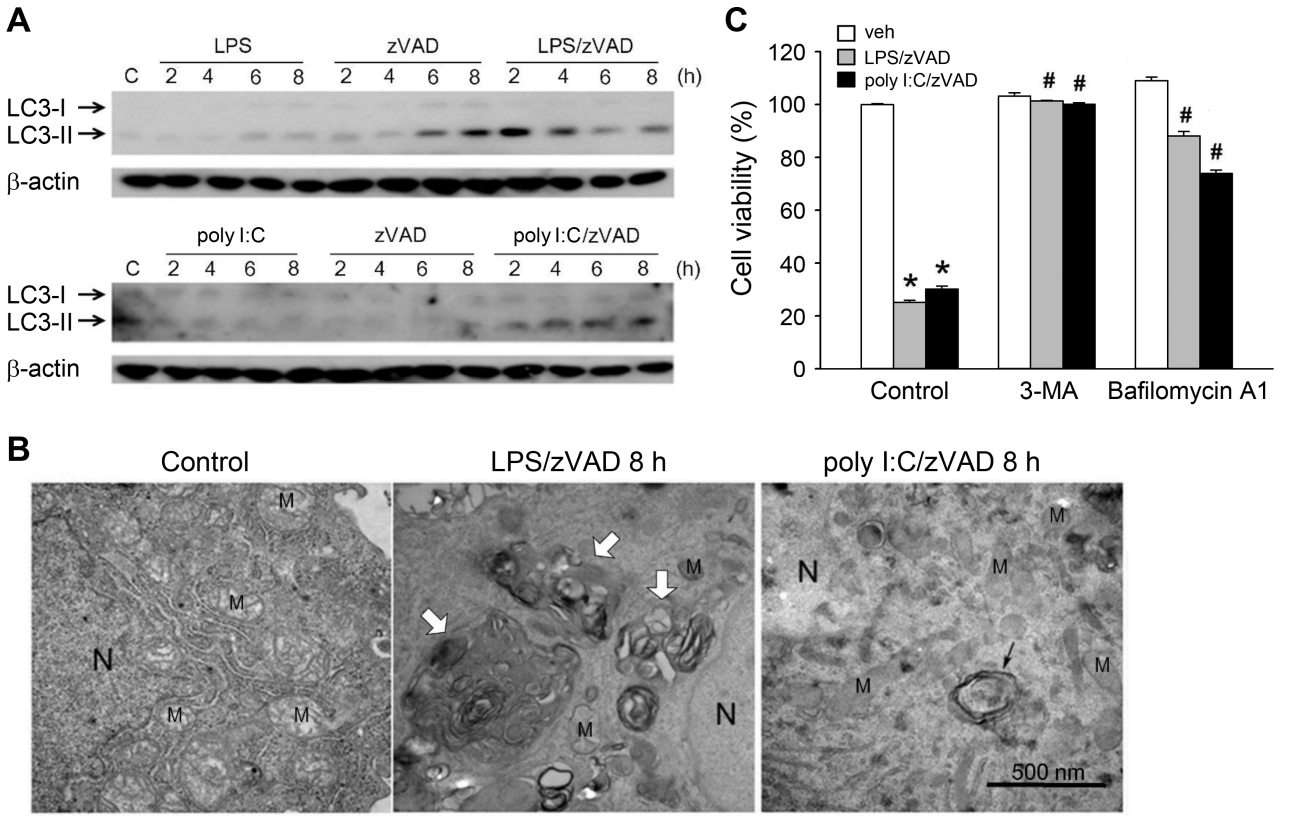

Fig. 2. zVAD/LPS and zVAD/poly I:C induce autophagic cell death in BMDMs. (A and B) BMDMs were pretreated with zVAD (20 μM) for 30 min prior to stimulation with LPS (1 μg/ml) or poly I:C (20 μg/ml) for different periods. The total cell lysates were subjected to SDS-PAGE and immunoblotting with LC3 antibody (A). In electron micrographs, BMDMs were conducted with 8 h drug treatment, either LPS/zVAD or poly I:C/zVAD, compared to control group. The white arrows indicate autolysosome, and the black arrow indicates the double membrane components, autophagosome. "N" indicates nuclei, "M" indicates mitochondria and the scale bar is 500 nm (B). (C) BMDMs were pretreated with zVAD (20 μM), 3-MA (1 mM), and/or bafilomycin A1 (100 nM) for 30 min, followed by the stimulation with LPS (1 μg/ml) or poly I:C (20 μg/ml). After treatment for 24 h, the cell viability was assessed by MTT assay. veh, vehicle. Data were the mean ± SEM from at least three independent experiments. $*P < 0.05$, indicating significant cytotoxic effects. $^{\#}P < 0.05$, indicating significant effect of 3-MA and bafilomycin A1 to inhibit cytotoxicity induced by zVAD/TLR ligands.

TLRs is involved in evoking necroptosis under conditions of caspase inhibition.

To determine whether autophagy is induced and contributes to cell necroptosis in zVAD/LPS- and zVAD/poly I:C-treated BMDMs, we examined the autophagic marker LC3-II, which is converted from LC3-I during the initiation of autophagy. Results revealed that within 8 h of treatment, LPS/zVAD and poly I:C/zVAD synergistically increased LC3-II levels. Compared with the weak effects of TLR3/4 ligands, zVAD alone induced a more apparent induction of LC3-II (Fig. 2A). Consistently, we found that zVAD can also induce morphological autophagic features in TLR3/4-activated BMDMs. Compared with the control, 8 h treatment with LPS/zVAD or poly I:C/zVAD induced the formation of a double membrane component, autolysosome (white arrows), and autophagosome (black arrow) (Fig. 2B). During the autophagic process, the morphology of the mitochondria was not affected by agent treatment (Fig. 2B). Notably, LPS/zVAD- and poly I:C/zVAD-induced cell death was blocked by 3-methyladenine (3-MA) and bafilomycin A1, two autophagy inhibitors (Wu et al., 2011) (Fig. 2C). These results suggest that autophagic cell death contributes to necroptosis in BMDMs treated with LPS/zVAD or poly I:C/zVAD.

zVAD differentially regulates LPS- and poly I:C-induced signaling pathways: No effects on JNK, p38, and IKK, while inhibition of ERK and Akt, and stimulation of IRF3 and STAT1 are observed

After observing that zVAD and TLR ligands exerted a synergistic effect on cell death, we examined the signaling cascades under combination treatment. We found that zVAD did not affect LPS- and poly I:C-induced activation of JNK, p38, or IKK. However, LPS- and poly I:C-activated ERK and Akt were inhibited by zVAD (Figs. 3A and 3B). On the other hand, TLR3 and TLR4 activate the TRIF-dependent IRF3 pathway to induce type I IFN production, which then functions in an autocrine manner to activate STAT1 phosphorylation. Here, we found that LPS and poly I:C induced the activation of IRF3 and STAT1, and zVAD can further enhance both responses upon co-treatment with LPS (Fig. 3C) or poly I:C

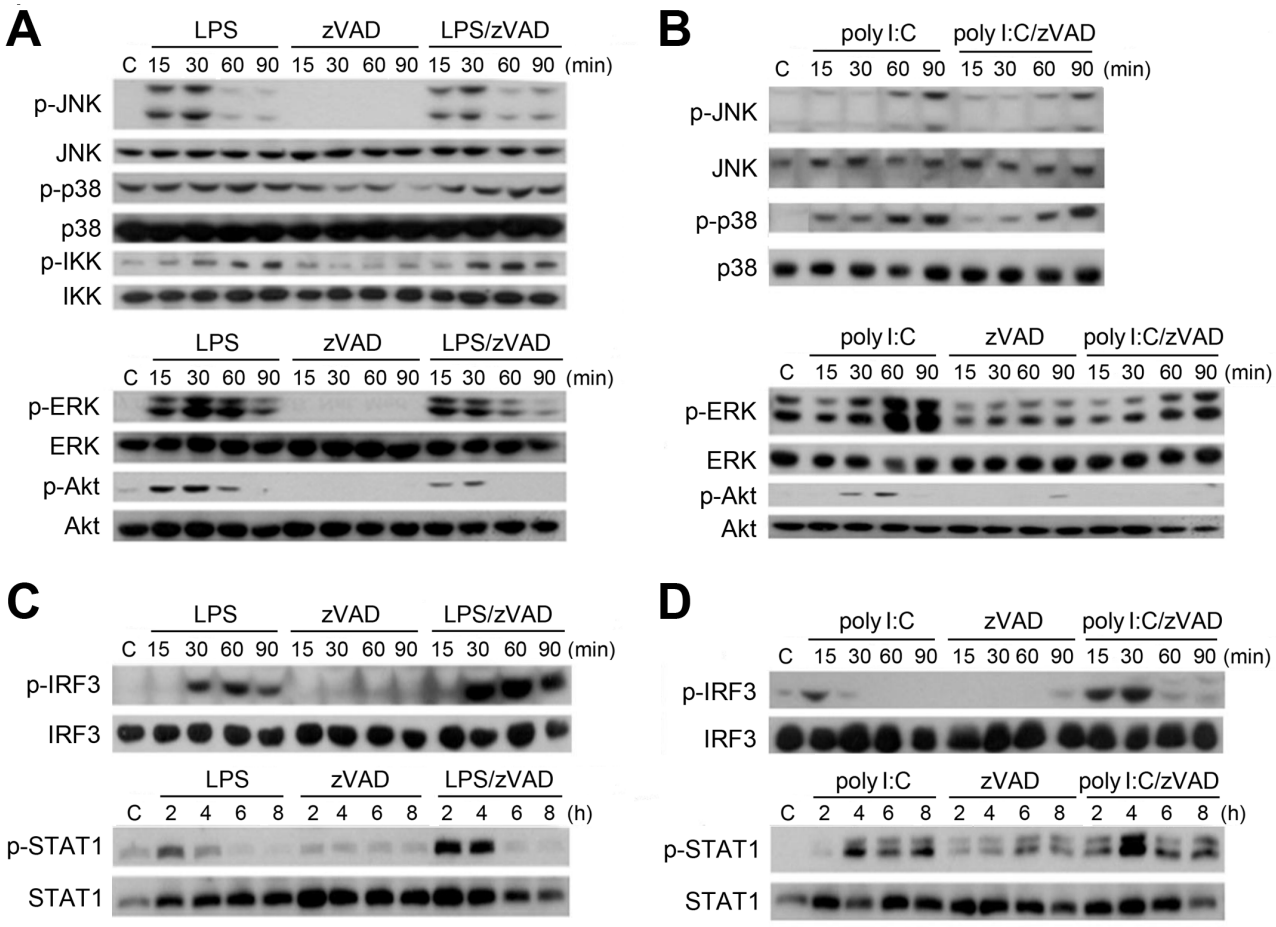

Fig. 3. zVAD differentially affects LPS- and poly I:C-induced signaling pathways: Inhibition of ERK and Akt, and enhancement of IRF3-STAT1 pathway, but no effects on IKK, JNK, and p38. BMDMs were pretreated with zVAD (20 μM) for 30 min prior to stimulation with LPS (1 μg/ml) (A and C) or poly I:C (20 μg/ml) (B and D). After incubation for different periods as indicated, the total cell lysates were subjected to SDS-PAGE followed by immunoblotting for JNK, p38, IKK, ERK, Akt (A and B), IRF3, and STAT1 (C and D). The results were representative traces that were repeated in three independent experiments.

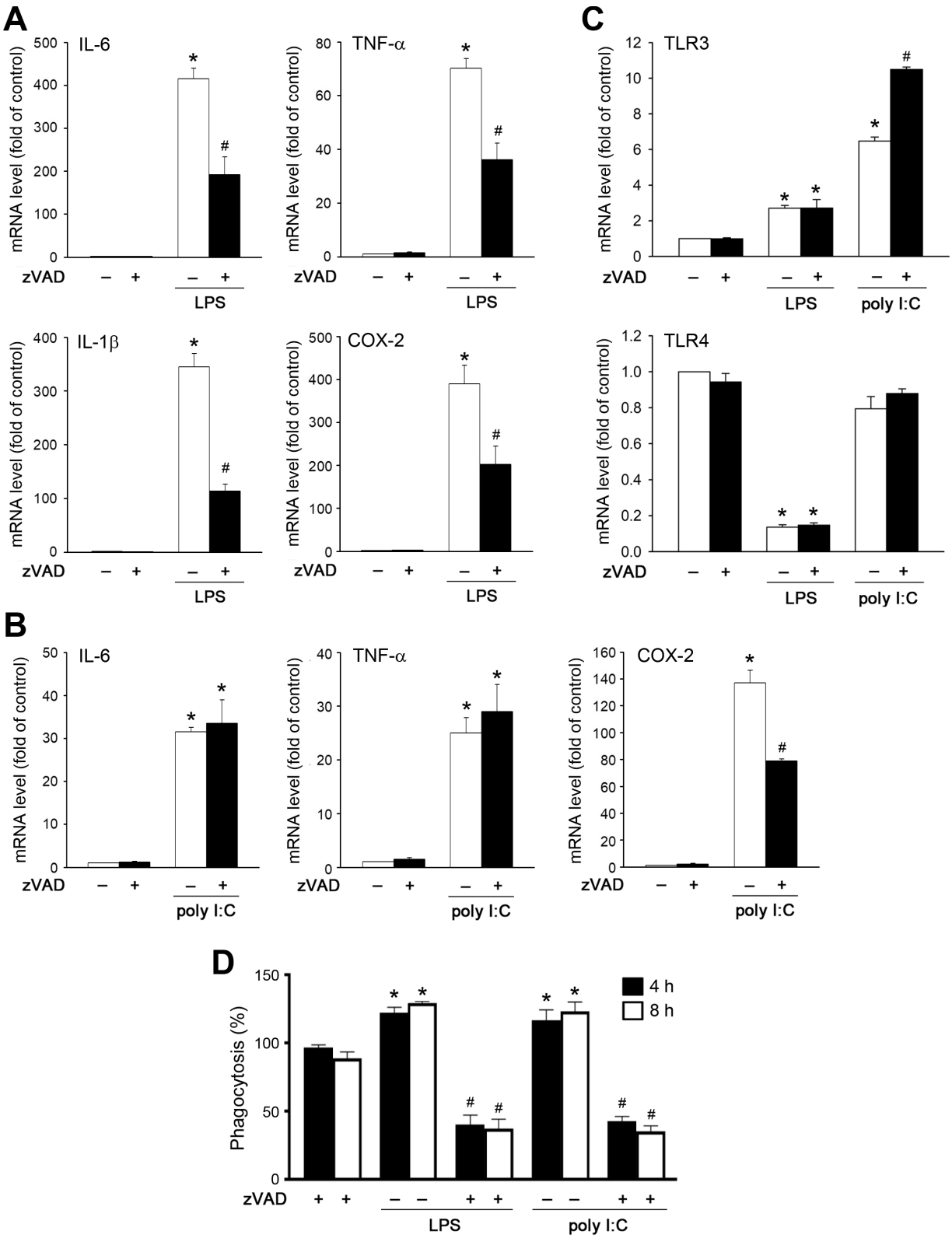

Fig. 4. Effects of zVAD on LPS- and poly I:C-induced inflammatory gene expression and phagocytosis. (A-C) BMDMs were pretreated with zVAD (20 μM) prior to treatment with LPS (1 μg/ml) or poly I:C (20 μg/ml) for 6 h. Real time-PCR was conducted to measure gene expression. (D) Cells were treated with agents as mentioned above for 4 h and 8 h. *E. coli* bioparticles were treated at the last one hour. Phagocytosis was determined by flow cytometry. Data were the mean ± SEM from at least three independent experiments. $*P < 0.05$, indicating significant effects of TLR ligands. $^{\#}P < 0.05$, indicating significant effect of zVAD to inhibit the effects of TLR ligands.

(Fig. 3D). These findings suggest that zVAD can enhance the TLR3/4-mediated TRIF-IRF3 signaling pathway.

Effects of zVAD on LPS- and poly I:C-induced inflammatory gene expression and phagocytosis

Next, we determined the pro-inflammatory gene expression induced by LPS and poly I:C. We found that LPS-induced IL-6, IL-1β, TNF-α, and COX-2 gene expression at 6 h was attenuated by zVAD (Fig. 4A). On the other hand, poly I:C treatment at 20 μg/ml upregulated moderate IL-6, TNF-α and COX-2 gene expression as compared to LPS (Fig. 4B), but did not significantly induce IL-1β gene expression (data not shown). Notably, zVAD only reduced the responses of COX-2 under poly I:C stimulation (Fig. 4B). Moreover, LPS and poly I:C can upregulate TLR3 gene expression with a higher effect of poly I:C than LPS. In contrast, LPS, but not poly I:C, can downregulate TLR4 mRNA levels. zVAD treatment further enhanced poly I:C-induced TLR3 gene expression, but did not alter the effects of LPS on the increase and inhibition of TLR3 and TLR4 gene expression, respectively (Fig. 4C).

Because phagocytosis is the innate immune response of macrophages, we also determined the effect of zVAD on cell phagocytosis. As previously described, LPS and poly I:C increased macrophage phagocytosis, while the effects of both TLR agonists were blocked by co-treatment with zVAD (Fig. 4D).

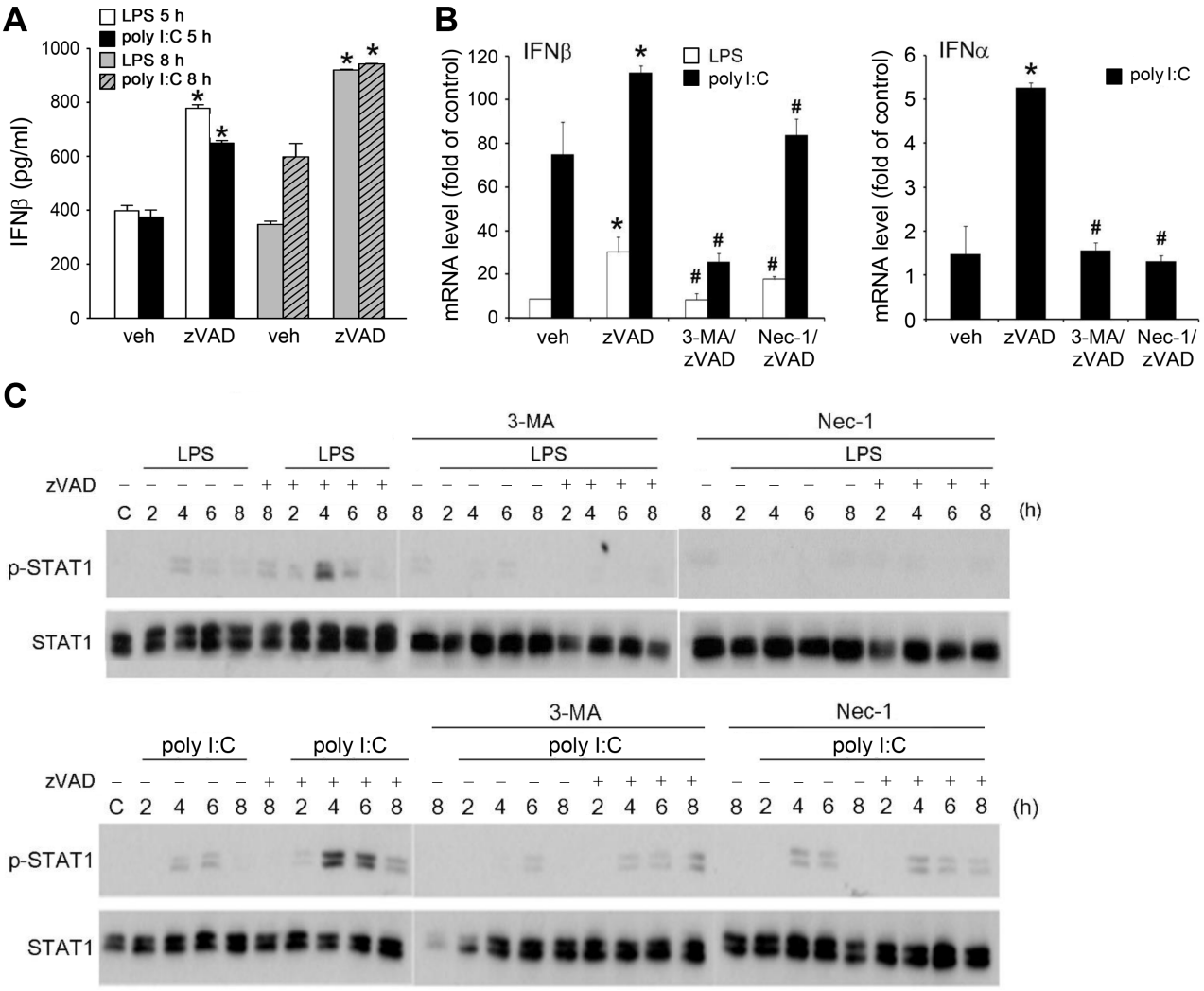

Fig. 5. RIP1 positively regulates IFN expression and STAT1 signaling. (A) BMDMs were pretreated with zVAD (20 μM) prior to treatment with LPS (1 μg/ml) or poly I:C (20 μg/ml) for 5 or 8 h. After incubation soluble IFNβ in culture medium was measured with commercial mouse IFNβ ELISA kit. (B) BMDMs were pretreated with zVAD (20 μM) either in the absence or presence of Nec-1 (10 μM) or 3-MA (1 mM) prior to the treatment with LPS (1 μg/ml) or poly I:C (20 μg/ml). After incubation for 3 h, mRNA was extracted and reversely transcribed for qPCR analyses of IFNβ and IFNα gene expression. Values were normalized to β-actin gene expression and expressed relative to the control group. Data were the mean ± SEM from at least three independent experiments. $*P < 0.05$, indicating significant enhancement of IFNs expression in the presence of zVAD. $^{\#}P < 0.05$, indicating significant effects of 3-MA and Nec-1 to inhibit IFNs expression induced by zVAD/TLR ligands. (C) Similar procedure as (B) was applied, and STAT1 phosphorylation at different time points was determined by immunobloting.

RIP1-dependent increases of IFNβ production and JAK/STAT1 signaling

After observing the ability of zVAD to enhance TRIF-mediated IRF3 signaling, we verified whether the major cytokine produced via this pathway (i.e., type I IFNs, especially IFNβ) is concomitantly increased. Additionally, because Nec-1, 3-MA, and bafilomycin A1 can prevent necroptosis, as shown in Figs. 1 and 2, we aimed to understand the effects of both agents on the TRIF-mediated signaling pathway. First, we collected the culture medium and measured the IFNβ expression. In the resting state with zVAD treatment alone, we could not detect the cytokine levels in the medium (data not shown). Howev-

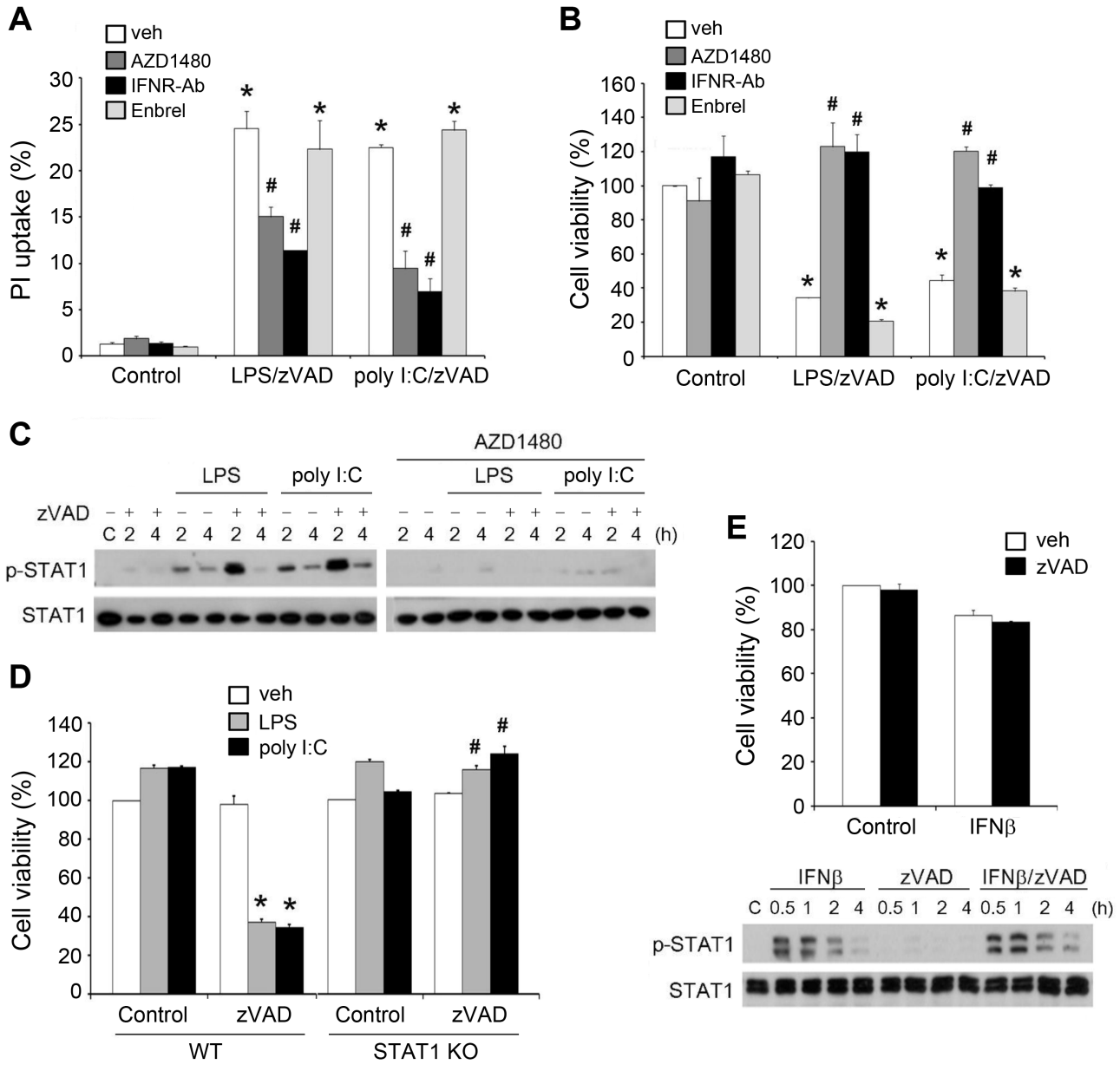

Fig. 6. IFNβ mediates cell necroptosis under LPS/zVAD and poly I:C/zVAD treatment. (A-C) BMDMs were pretreated with zVAD (20 μM), AZD1480 (1 μM), IFNR-Ab (1 μg/ml) or Embrel (10 ng/ml) for 30 min and stimulated with LPS (1 μg/ml) or poly I:C (20 μg/ml). After incubation for 24 h, cell viability was determined by PI uptake (A) and MTT assay (B). In some experiments, STAT1 phosphorylation was determined by immunobloting at different periods (C). (D) The wild type and STAT1 knockout BMDMs were pretreated with zVAD (20 μM) for 30 min prior to LPS (1 μg/ml) or poly I:C (20 μg/ml) stimulation. After 24 h incubation, the cell viability was assessed by MTT assay. (E) BMDMs were pretreated with zVAD (20 μM) for 30 min prior to IFNβ (10 ng/ml) stimulation. Cell viability was determined by MTT assay after 24 h incubation (upper panel), and STAT1 activation status was determined at different periods of time as indicated (lower panel). veh, vehicle. Data were the mean ± SEM from at least three independent experiments. $^{*}P < 0.05$, indicating significant effects of zVAD/TLR ligands on cell viability. $^{\#}P < 0.05$, indicating significant reversal effects of AZD1480, IFNR-Ab and STAT1 KO on cytotoxicity induced by zVAD/TLR ligands.

er, we found that zVAD enhanced LPS- and poly I:C-induced IFNβ release at 5 h and 8 h (Fig. 5A). Accordingly, the mRNA level of IFNβ was upregulated by LPS and poly I:C with higher efficacy of poly I:C, and both responses were further increased in the presence of zVAD. For IFNα mRNA expression, only poly I:C slightly upregulated gene transcription (Fig. 5B), while LPS did not exert this effect (data not shown). Likewise, zVAD further increased IFNα gene expression under poly I:C treatment (Fig. 5B). Moreover, these increased responses of zVAD to IFNα and IFNβ expression were inhibited by Nec-1 and 3-MA (Fig. 5B). In agreement with the effects of decreasing IFN expression, 3-MA and Nec-1 can reduce the stimulated STAT1 phosphorylation caused by LPS/zVAD and poly I:C/zVAD (Fig. 5C). These results suggest that zVAD can enhance TRIF-dependent IFN expression and STAT1 signaling, and both actions rely on RIP1 kinase activation.

Autocrine IFNβ involves in cell death via JAK-STAT1 pathway

After observing the increased IFNβ production, we examined the contribution of type I IFNs to LPS/zVAD- and poly I:C/zVAD-induced cell death. To this end, we used a neutralizing antibody of type I IFN receptor (IFNR-Ab) and JAK inhibitor AZD1480 to manipulate endogenous IFN function and signaling, respectively. Using PI uptake and MTT assay as indices of cell death, we found that treatment with IFNR-Ab or AZD1480 decreased LPS/zVAD- and poly I:C/zVAD-induced necroptosis (Figs. 6A and 6B). Meanwhile, AZD1480 was found to decrease STAT1 activation induced by LPS and poly I:C, even in the presence of higher phospho-STAT1 expression under zVAD pretreatment (Fig. 6C). Notably, we found that necroptotic cell death was abrogated in STAT1 knockout BMDMs (Fig. 6D). Therefore, we suggest that RIP1-dependent necroptotic cell death caused by TLR ligands/zVAD co-treatment in macrophages relies on autocrine JAK/STAT1 signaling of IFNR.

To further address this notion, we determined the effects of exogenous IFNβ treatment. IFNβ treatment, either alone or in combination with zVAD, failed to change the viability of BMDMs (Fig. 6E, upper panel). In addition, IFN-induced

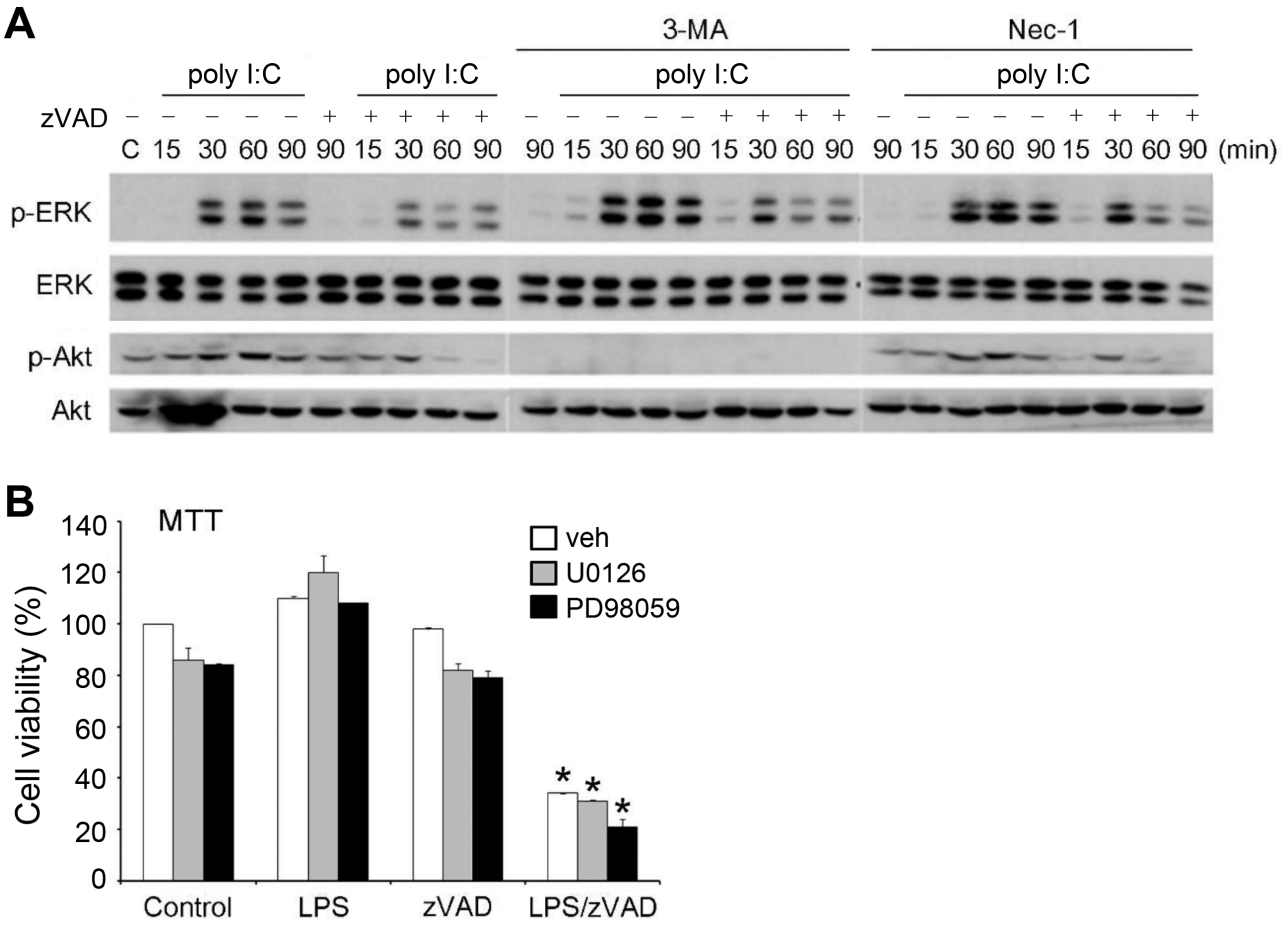

Fig. 7. ERK and Akt inhibition are not mediated by RIP1 and not involved in necroptosis. (A) BMDMs were pretreated with zVAD (20 μM) in the absence or presence of 3-MA (1 mM) or Nec-1 (10 μM) for 30 min and then treated with poly I:C (20 μg/ml). After incubation for different periods as indicated, the total cell lysates were subjected to SDS-PAGE followed by immunoblotting for ERK and Akt. (B) BMDMs were pretreated with U0126 (3 μM) or PD98059 (10 μM) for 30 min and then treated with LPS (1 μg/ml) and/or zVAD (20 μM). After 24 h, the cell viability was determined by MTT assay. veh, vehicle. Data were the mean ± SEM from at least three independent experiments. $*P < 0.05$, indicating synergistic cell death caused by LPS and zVAD.

STAT1 phosphorylation was not affected by zVAD (Fig. 6E, lower panel). These results suggest that RIP1-depednent signaling for enhancing IFNβ production is a prerequisite modulator of cell necroptosis; however, IFNβ itself is not sufficient to induce this event even in the presence of zVAD. This implies that events downstream of the TRIF-RIP1 pathway beyond STAT1 activation are necessary to integrate death mechanisms for cell necroptosis.

In addition to IFNs, we considered the possible involvement of TNF-α in necroptosis. The reason for this speculation is based on previous studies showing that TNF-α can trigger necroptosis in mouse embryonic fibroblasts (Lin et al., 2004) and L929 fibrosarcoma cells (Vandenabeele et al., 2010b). Moreover, the autocrine action of TNF-α is involved in zVAD-induced cell necrosis in L929 cells (Chen et al., 2011; Wu et al., 2011). To address this possibility, we treated BMDMs with a TNFα neutralizing antibody, Embrel (10 ng/ml). We found that cell death caused by zVAD/LPS and zVAD/poly I:C was unaffected in the presence of Embrel (Figs. 6A and 6B).

RIP-1 independent inhibition of Akt and ERK signaling might not involve in LPS/zVAD-induced cell necroptosis

Next, we investigated whether zVAD-mediated ERK and Akt inhibition, as shown in Fig. 3, might contribute to RIP1-dependent death. First, we found that 3-MA itself did not affect EKR activity, but enhanced poly I:C-induced ERK phosphorylation. Under these conditions, zVAD reduced the increase in ERK phosphorylation under TLR3 activation (Fig. 7A). Unsurprisingly, 3-MA, a dual inhibitor of class I and class III PI3Ks (Lin et al., 2012; Wu et al., 2010), abrogated Akt activation under poly I:C stimulation. For Nec-1, we found that it failed to alter ERK and Akt activation caused by poly I:C or the inhibitory effects of zVAD on both signals (Fig. 7A). These results suggest that zVAD-induced ERK and Akt inhibition occurs through a mechanism independent of RIP1 kinase activation.

To understand whether ERK inhibition contributes to zVAD-induced necroptosis in TLR-activated BMDMs, we used pharmacological ERK inhibitors to determine cell viability. We found that the MEK inhibitor, U0126 or PD98059, did not alter the viability of BMDMs when treated with LPS and zVAD, regardless of individual treatment and co-treatment (Fig. 7B). These findings suggest that RIP1-independent ERK inhibition caused by zVAD/TLR ligands might not be involved in TLR ligands/zVAD-induced necroptosis in BMDMs. Because Nec-1 did not alter the inhibitory effect on Akt, we suggest that Akt inhibition might not contribute to cell death caused by TLR/zVAD.

ROS production participates in TLR/zVAD-induced autophagic cell necroptosis

ROS have been shown to participate in non-caspase-induced cell necrosis. We hypothesized that ROS play a crucial role in the necroptosis induced by zVAD plus TLR ligands. First, we used the antioxidant BHA to test cell viability. The results showed that BHA protected cells from death (Fig. 8A). Next, we measured intracellular ROS production using the $DCFH_2$-DA. We found that LPS alone significantly increased ROS production after 3 h of treatment and then gradually declined. In the presence of zVAD, the peak of ROS production at 3 h was enhanced and ROS level was still maintained at a higher level compared to control cells within 8-16 h (Fig. 8B). Of note, we only detected a slight increase in the effect of poly I:C on cytosolic ROS production, which was only about a 15% increase at 3 h. At 1 h and 6 h after poly I:C (20 μg/ml) treatment, the cytosolic ROS level did not change (data not shown). Due to the marginal effect on ROS, we did not observe any significant effect of zVAD. We speculate that these data for poly I:C might result from the weaker effect of poly I:C than LPS and the low sensitivity of ROS detection. Next, we used Nec-1, AZD1480, and IFNR-Ab to examine whether the RIP1-IFN-JAK-STAT1 pathway is associated with ROS regulation. The results revealed that the LPS/zVAD-induced increase in ROS at 3, 8, and 12 h was inhibited by all manipulations (Fig. 8C). Moreover, the elevated ROS production by LPS, either in the absence or presence of zVAD, was abrogated in STAT1 knockout BMDMs (Fig. 8D). Therefore, it is suggested that elevated ROS production resulting from the RIP1/IFNβ/JAK/STAT1 pathway participates in LPS/zVAD-induced cell death.

Given that both autophagic cell death (Fig. 2C) and ROS production (Fig. 8A) are responsible for necroptosis, we attempted to further understand the link between these events. Using LC3-II conversion as an index of autophagic induction, we found that LPS/zVAD- and poly I:C/zVAD-elicited LC3-II expression was attenuated by BHA (Fig. 9A). Similarly, Nec-1 was effective in attenuating the action of LPS/zVAD (Fig. 9B, upper panel). In contrast, U0126 had no effect on this event (Fig. 9B, lower panel). Moreover, BMDMs deficient in STAT1 also displayed less autophagic induction than WT cells (Fig. 9C). These data suggest that ROS are involved in TLR ligands/zVAD-induced autophagy.

DISCUSSION

The caspase inhibitor, zVAD, has been shown not only to protect cells from apoptosis but also to induce caspase-independent cell necroptosis. Moreover, zVAD can also enhance autophagic cell death in TLR-activated macrophages (Martinet et al., 2006; Xu et al., 2006, 2007). In this study, we confirmed this notion in simultaneous TLR3/4-activated and zVAD-treated BMDMs by observing the increased LC3-II expression and the appearance of autophagosomes and autolysosomes by electronic microscopy. In addition, we demonstrated that LPS/zVAD or poly I:C/zVAD-induced cell death in BMDMs can be protected by the autophagy inhibitors 3-MA and bafilomycin A1, suggesting autophagic death of BMDMs under TLR/zVAD stimulation. This suggests that autophagy might coordinate with necroptosis in zVAD-induced cell death in TLR-activated BMDMs. In addition, we found that TRIF-RIP1-dependent autocrine action of IFNβ may participate in the process of zVAD-induced autophagic and necroptotic death in TLR3- and TLR4-activated macrophages via the JAK/STAT1/ROS pathway.

The downstream of TLR4 contains two pathways: MyD88-dependent and TRIF-dependent. Although both signaling pathways have been demonstrated for TLR-mediated

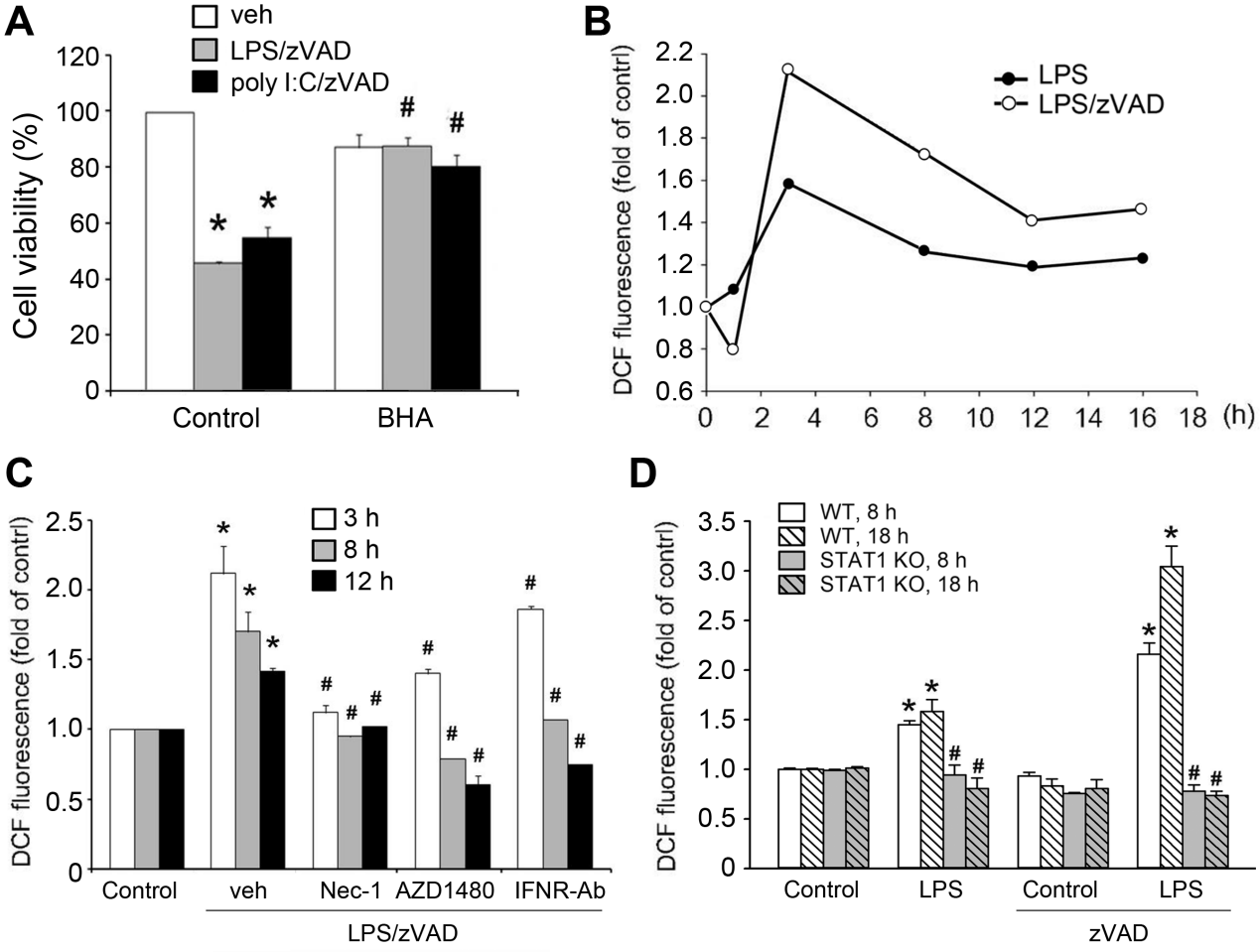

Fig. 8. ROS production resulting from STAT1 activation contributes to necroptosis. (A) BMDMs were pretreated with BHA (100 μM) and/or zVAD (20 μM) for 30 min prior to LPS (1 μg/ml) or poly I:C (20 μg/ml) treatment. After incubation for 24 h, the cell viability was assessed by MTT assay. (B) Cells were pretreated with zVAD, LPS (1 μg/ml) and/or poly I:C for different periods, and then intracellular ROS was measured by $DCFH_2$-DA fluorescence. (C) Similar experiments as (B) were conducted in cells treated with Nec-1 (10 μM), AZD1480 (1 μM) or IFNR-Ab (1 μg/ml). veh, vehicle. (D) BMDMs from WT and STAT1 KO mice were treated with zVAD and/or LPS, and ROS levels at 8 h and 18 h were measured. Data were the mean ± SEM from at least three independent experiments. $*P < 0.05$, indicating enhancement effects of zVAD on cytotoxicity and ROS production. $^{\#}P < 0.05$, indicating reversal effects of BHA, Nec-1, AZD1480, IFNR-Ab, and STAT1 knockout on zVAD-induced cytotoxicity and ROS production.

autophagy (Shi and Kehrl, 2008), the TRIF-RIP1 pathway is more widely recognized after zVAD treatment. As reported, caspase-1-dependent RIP1 cleavage inhibits autophagy; conversely, zVAD can induce autophagy by increasing downstream signaling of RIP1 (Jabir et al., 2014). Here, our study indicates that the TRIF-dependent IRF3 pathway shared by TLR3 is enhanced by zVAD. Accordingly, the subsequent increase in type I IFNα/β production and its autocrine action via IFNR to trigger JAK-STAT1 signaling were enhanced by zVAD.

Type I IFNs play important roles in innate immune and adaptive immune responses by inducing the transcription of a select set of genes called IFN-stimulated genes. In this study, confirming previous findings (Legarda et al., 2016; McComb et al., 2014), we demonstrated the essential role of IFNs in LPS/zVAD- and polyIC/zVAD-induced cell death. The evidence for this conclusion includes the ability of neutralizing antibodies against IFNR, JAK inhibitor AZD1480, and genetic STAT1 knockout to prevent cell death. Previously, STAT1 was shown to be involved in LPS/zVAD-induced cell death in macrophages (Kim and Lee, 2005). In this study, we provide more comprehensive evidence to link previous findings from TRIF-RIP1 to IFN production and then to autocrine IFNR-JAK-STAT1 actions for ROS production and subsequent cell death. Despite the essential role of IFNs-JAK-STAT1 in TLR ligand/zVAD-induced cell death, exogenous βIFN-γ/zVAD co-treatment did not induce cell death, and zVAD did not affect STAT1 phosphorylation caused by IFNβ. This suggests that events downstream of the TRIF-RIP1 pathway besides the IFNs-JAK-STAT1 axis is a prerequisite for integrating death mechanisms for autophagic cell necroptosis.

In our results, LPS and poly I:C induced p38, JNK, ERK, Akt, and IKK activation. However, only ERK and Akt phosphory-

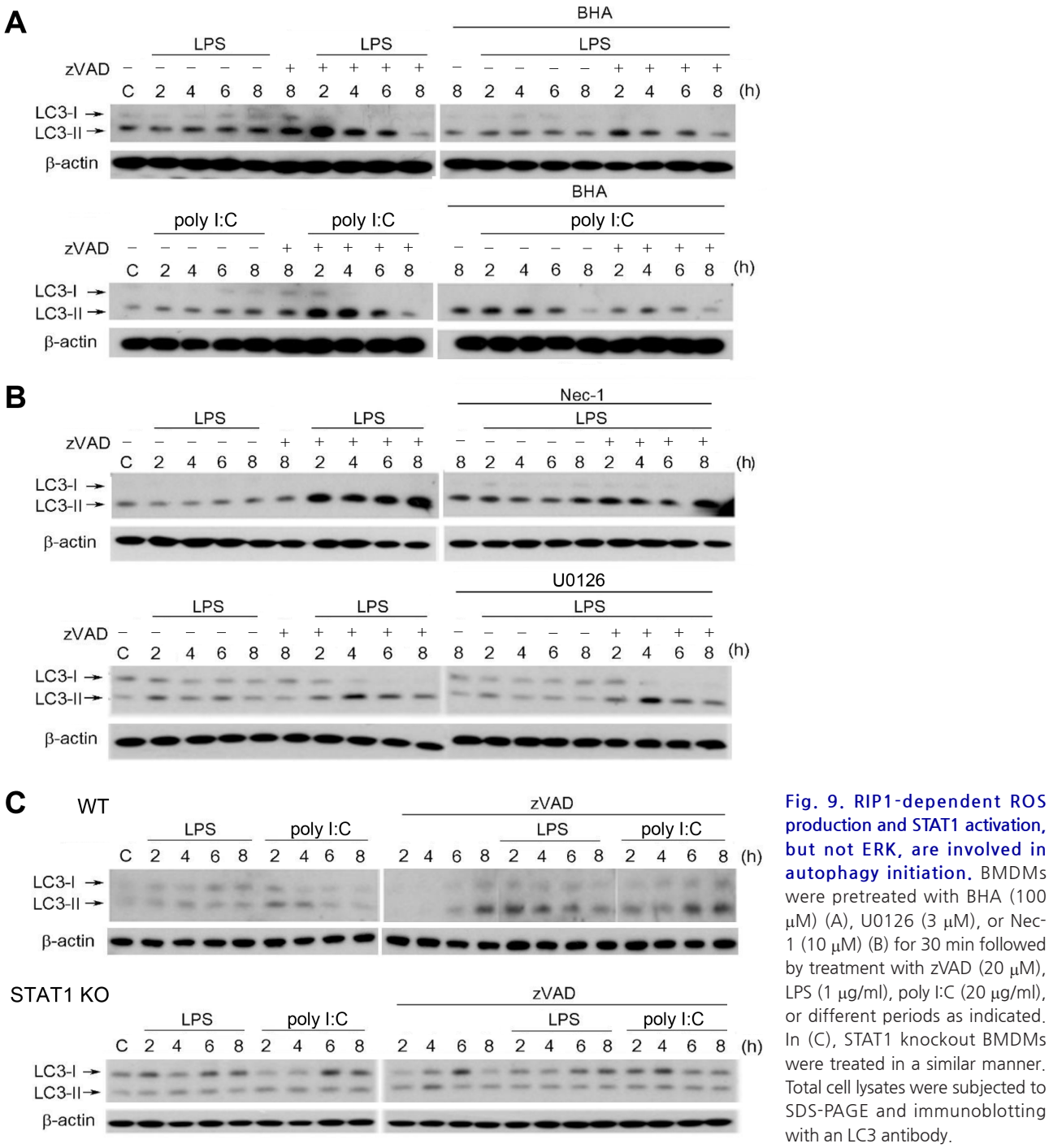

Fig. 9. RIP1-dependent ROS production and STAT1 activation, but not ERK, are involved in autophagy initiation. BMDMs were pretreated with BHA (100 μM) (A), U0126 (3 μM), or Nec-1 (10 μM) (B) for 30 min followed by treatment with zVAD (20 μM), LPS (1 μg/ml), poly I:C (20 μg/ml), or different periods as indicated. In (C), STAT1 knockout BMDMs were treated in a similar manner. Total cell lysates were subjected to SDS-PAGE and immunoblotting with an LC3 antibody.

lation were inhibited by zVAD. Although we still do not have detailed molecular mechanisms for the distinct actions of zVAD on TLR signals via MyD88 and TRIF, our data exclude the involvement of ERK and Akt inhibition in cell death. This is because the ERK inhibitor U0126 and MEK inhibitor PD98059 did not mimic the action of zVAD to induce cell death in TLR-activated BMDMs. Undeniably, as we mentioned above for the situation of IFNs, we still need to consider other death elements that might orchestrate or leverage a more complicated death mechanism by interacting with ERK.

In the TRIF-dependent pathway, RIP1 and TBK/IRF3 are divided into two pathways. TBK/IRF3 can regulate the inflammatory response to produce cytokines, such as type I IFNs (Schmalz et al., 2011). On the other hand, RIP1 is at the crossroad position to control cell fate (Witt and Vucic, 2017). It can activate IKK-NF-B to regulate cell viability (Meylan et al., 2004; Schmalz et al., 2011; Takeda et al., 2003), but can also induce necrosis in the absence of caspase activity (Jabir et al., 2014; Kaiser et al., 2013; Seya et al., 2012; Xu et al., 2006, 2007). In this study, we found that RIP1 inhibitor does not

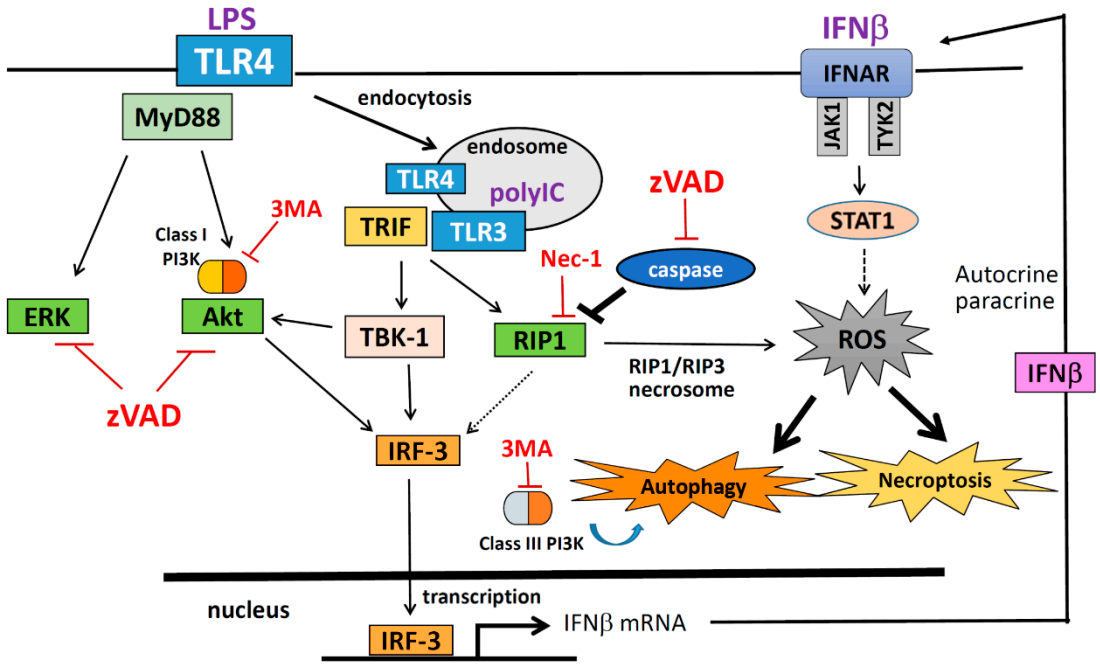

Fig. 10. Signaling pathway and molecular mechanisms underlying TLR/zVAD-induced autophagic cell necroptosis. In TLR3/4 activated macrophages, TRIF-mediated RIP1/IRF3 and RIP1/RIP3 signaling pathways are enhanced by the caspase inhibitor zVAD, leading to IFN production and necrosome formation, respectively. Autocrine IFNR-JAK-STAT1 action further increases ROS production, which is a prerequisite for autophagic cell necroptosis. zVAD also inhibits LPS- and poly I:C-elicited ERK and Akt activation, both of which are not involved in the cell death mechanism.

alter polyIC-induced Akt activation but can suppress zVAD-induced enhancement of IFN expression, phospho-STAT1 expression, and cell death. Taken together, we suggest that the RIP1 pathway downstream of TRIF controls IRF3 activation for IFN expression and subsequent cell death in zVAD/TLR-treated macrophages.

ROS play an essential role in caspase-independent cell death in many different cell systems. NADPH oxidase, an important mediator of ROS production, is involved in TLR-mediated signaling pathways, including NF-kB for innate immunity (Liu et al., 2015). ROS also participates in zVAD-induced non-apoptotic autophagic cell death in RAW 264.7 macrophages (Xu et al., 2006). In our previous study, we found that in mouse embryonic fibroblasts, zVAD plus Fas ligand induced non-apoptotic necrosis with the production of ROS (Chen et al., 2009). Herein, we found that zVAD can enhance LPS-induced ROS production, and BHA can protect BMDMs from zVAD-induced autophagic cell necroptosis upon LPS and poly I:C stimulation. Unexpectedly, we only detected a slight increase (15%) in cytosolic ROS within 6 h of treatment with poly I:C. We speculate that this effect different from LPS might be due to the limitation of detection sensitivity of the ROS dye. Despite this effect, the protective effect of BHA on cell death caused by poly I:C/zVAD suggests the involvement of ROS in cell death resulting from autophagy and necroptosis.

Moreover, zVAD-enhanced ROS production in TLR-activated BMDMs was inhibited by Nec-1, AZD1480, and IFNR neutralizing antibodies as well as by STAT-1 knockout. These findings suggest that zVAD-induced ROS production is regulated by the RIP1 and IFN/JAK/STAT pathways in TLR-activated BMDMs. Apart from ROS-dependent STAT1 activation (Liu et al., 2017), STAT1 seems to control ROS in a positive feedback manner, although the detailed mechanism is not clear (Kim et al., 2017). Moreover, we showed that ROS can mediate LC3-II expression under LPS/zVAD or poly I:C/zVAD treatment. Previously depending on the cell types and contexts ERK has been shown to induce (Chen et al., 2011) or inhibit autophagy (Gorentla et al., 2011; Wang et al., 2009). In this study, besides TRIF-RIP1 and STAT1-ROS axis, which participate in LC3-II expression, more detailed molecular mechanisms, especially in signaling integration and cytokine involvement, require further investigation.

In this study, we also found differential effects of zVAD on LPS- and poly I:C-induced inflammatory gene expression. zVAD significantly decreased LPS-induced IL-1β, IL-6, TNF α and COX-2 gene expression, while only COX-2 induction by poly I:C was reduced by zVAD. We also considered whether TLR receptor expression might contribute to these findings, and in particular, if the increased TRIF signaling pathway by zVAD results from the change in TLR3. We found that only LPS treatment could downregulate TLR4, and zVAD had no effect in this event. As for TLR3 mRNA, which is upregulated by LPS and poly I:C, zVAD only increased the effect of poly I:C. The finding that poly I:C has a higher effect than LPS on upregulation of TLR3 is consistent with previous studies (Chen et al., 2021; Pan et al., 2011). Although these findings might partially support our observation that zVAD can enhance poly I:C-induced signaling, this mechanism cannot be applied in the case of LPS. Therefore, the enhancement of

TRIF-mediated signaling by zVAD is a major contributor to cell death. The reason for the effect of LPS on increasing TLR3 gene expression was not changed by zVAD requires further investigation. In addition, the differential effects of zVAD on TLR3- and TLR4-mediated inflammatory gene expression imply that more complicated mechanisms are involved in the expression of these genes. We observed that the signaling pathways of TLR3/TLR4 are differentially affected by zVAD, which does not affect IKK, p38, or JNK but inhibits ERK and Akt. Therefore, crosstalk between signaling pathways and differential regulatory roles of signaling molecules and transcription factors for individual genes are suggested for the effects of zVAD on gene regulation.

In summary, caspase inhibition by zVAD enhanced LPS- and poly I:C-induced autophagic cell necroptosis in macrophages. TRIF-dependent RIP1 activation contributes to type I IFN production, and autocrine signaling of JAK-STAT1 contributes to ROS production, autophagy, and cell necroptosis. A summary graph of this study is shown in Fig. 10.

ACKNOWLEDGMENTS

This work was supported by the Ministry of Science and Technology (108-2320-B-002-028-MY3), National Taiwan University Hospital Yunlin Branch (NTUHYL110.S021), and National Taiwan University (110L890501). We thank the STAT1 knockout mice from Dr. Chien-Kuo Lee (Graduate Institute of Immunology, National Taiwan University College of Medicine).

AUTHOR CONTRIBUTIONS

W.W.L. designed the experiments and analyzed the results. Y.S.C., W.C.C., H.N.K., C.Y.C., D.Y.H., and P.S. performed the experiments and analyzed the results. W.W.L. wrote the manuscript.

CONFLICT OF INTEREST

The authors have no potential conflicts of interest to disclose.

ORCID

Yuan-Shen Chen https://orcid.org/0000-0001-8215-7041
Wei-Chu Chuang https://orcid.org/0000-0001-8181-1099
Hsiu-Ni Kung https://orcid.org/0000-0001-6979-8346
Ching-Yuan Cheng https://orcid.org/0000-0001-9251-7549
Duen-Yi Huang https://orcid.org/0000-0002-2787-1346
Ponarulselvam Sekar https://orcid.org/0000-0003-4282-2865
Wan-Wan Lin https://orcid.org/0000-0002-3207-734X

REFERENCES

Bonapace, L., Bornhauser, B.C., Schmitz, M., Cario, G., Ziegler, U., Niggli, F.K., Schäfer, B.W., Schrappe, M., Stanulla, M., and Bourquin, J.P. (2010). Induction of autophagy-dependent necroptosis is required for childhood acute lymphoblastic leukemia cells to overcome glucocorticoid resistance. J. Clin. Invest. *120*, 1310-1323.

Chen, C.Y., Hung, Y.F., Tsai, C.Y., Shih, Y.C., Chou, T.F., Lai, M.Z., Wang, T.F., and Hsueh, Y.P. (2021). Transcriptomic analysis and C-terminal epitope tagging reveal differential processing and signaling of endogenous TLR3 and TLR7. Front. Immunol. *12*, 686060.

Chen, S.Y., Chiu, L.Y., Ma, M.C., Wang, J.S., Chien, C.L., and Lin, W.W. (2011). zVAD-induced autophagic cell death requires c-Src-dependent ERK and JNK activation and reactive oxygen species generation. Autophagy *7*, 217-228.

Chen, T.Y., Chi, K.H., Wang, J.S., Chien, C.L., and Lin, W.W. (2009). Reactive oxygen species are involved in FasL-induced caspase-independent cell death and inflammatory responses. Free Radic. Biol. Med. *46*, 643-655.

Denton, D. and Kumar, S. (2019). Autophagy-dependent cell death. Cell Death Differ. *26*, 605-616.

Dey, A., Mustafi, S.B., Saha, S., Dwivedi, S.K.D., Mukherjee, P., and Bhattacharya, R. (2016). Inhibition of BMI1 induces autophagy-mediated necroptosis. Autophagy *12*, 659-670.

Doherty, J. and Baehrecke, E.H. (2018). Life, death and autophagy. Nat. Cell Biol. *20*, 1110-1117.

Galluzzi, L., Kepp, O., Chan, F.K., and Kroemer, G. (2017). Necroptosis: mechanisms and relevance to disease. Annu. Rev. Pathol. *12*, 103-130.

Gao, T., Zhang, S.P., Wang, J.F., Liu, L., Wang, Y., Cao, Z.Y., Hu, Q.K., Yuan, W.J., and Lin, L. (2018). TLR3 contributes to persistent autophagy and heart failure in mice after myocardial infarction. J. Cell. Mol. Med. *22*, 395-408.

Gorentla, B.K., Wan, C.K., and Zhong, X.P. (2011). Negative regulation of mTOR activation by diacylglycerol kinases. Blood *117*, 4022-4031.

Grootjans, S., Vanden Berghe, T., and Vandenabeele, P. (2017). Initiation and execution mechanisms of necroptosis: an overview. Cell Death Differ. *24*, 1184-1195.

Hanson, B. (2016). Necroptosis: a new way of dying? Cancer Biol. Ther. *17*, 899-910.

He, S., Wang, L., Miao, L., Wang, T., Du, F., Zhao, L., and Wang, X. (2009). Receptor interacting protein kinase-3 determines cellular necrotic response to TNF-alpha. Cell *137*, 1100-1111.

Jabir, M.S., Ritchie, N.D., Li, D., Bayes, H.K., Tourlomousis, P., Puleston, D., Lupton, A., Hopkins, L., Simon, A.K., Bryant, C., et al. (2014). Caspase-1 cleavage of the TLR adaptor TRIF inhibits autophagy and beta-interferon production during *Pseudomonas aeruginosa* infection. Cell Host Microbe *15*, 214-227.

Kaiser, W.J., Sridharan, H., Huang, C., Mandal, P., Upton, J.W., Gough, P.J., Sehon, C.A., Marquis, R.W., Bertin, J., and Mocarski, E.S. (2013). Toll-like receptor 3-mediated necrosis via TRIF, RIP3, and MLKL. J. Biol. Chem. *288*, 31268-31279.

Khan, M.J., Rizwan Alam, M., Waldeck-Weiermair, M., Karsten, F., Groschner, L., Riederer, M., Hallström, S., Rockenfeller, P., Konya, V., Heinemann, A., et al. (2012). Inhibition of autophagy rescues palmitic acid-induced necroptosis of endothelial cells. J. Biol. Chem. *287*, 21110-21120.

Kim, H.S. and Lee, M.S. (2005). Essential role of STAT1 in caspase-independent cell death of activated macrophages through the p38 mitogen-activated protein kinase/STAT1/reactive oxygen species pathway. Mol. Cell. Biol. *25*, 6821-6833.

Kim, J.Y., Choi, G.E., Yoo, H.J., and Kim, H.S. (2017). Interferon potentiates Toll-like receptor-induced prostaglandin D2 production through positive feedback regulation between signal transducer and activators of yranscription 1 and reactive oxygen species. Front. Immunol. *8*, 1720.

Kim, S.J. and Li, J. (2013). Caspase blockade induces RIP3-mediated programmed necrosis in Toll-like receptor-activated microglia. Cell Death Dis. *4*, e716.

Kist, M. and Vucic, D. (2021). Cell death pathways: intricate connections and disease implications. EMBO J. *40*, e106700.

Lai, M., Yao, H., Shah, S.Z.A., Wu, W., Wang, D., Zhao, Y., Wang, L., Zhou, X., Zhao, D., and Yang, L. (2018). The NLRP3-caspase 1 inflammasome negatively regulates autophagy via TLR4-TRIF in prion peptide-infected microglia. Front. Aging Neurosci. *10*, 116.

Legarda, D., Justus, S.J., Ang, R.L., Rikhi, N., Li, W., Moran, T.M., Zhang, J., Mizoguchi, E., Zelic, M., Kelliher, M.A., et al. (2016). CYLD proteolysis protects macrophages from TNF-mediated auto-necroptosis induced by LPS and licensed by type I IFN. Cell Rep. *15*, 2449-2461.

Lin, Y., Choksi, S., Shen, H.M., Yang, Q.F., Hur, G.M., Kim, Y.S., Tran, J.H., Nedospasov, S.A., and Liu, Z.G. (2004). Tumor necrosis factor-induced nonapoptotic cell death requires receptor-interacting protein-mediated cellular reactive oxygen species accumulation. J. Biol. Chem. *279*, 10822-10828.

Lin, Y.C., Huang, D.Y., Chub, C.L., and Lin, W.W. (2010). Anti-inflammatory actions of Syk inhibitors in macrophages involve non-specific inhibition of toll-like receptors-mediated JNK signaling pathway. Mol. Immunol. *47*, 1569-1578.

Lin, Y.C., Kuo, H.C., Wang, J.S., and Lin, W.W. (2012). Regulation of inflammatory response by 3-methyladenine involves the coordinative actions on Akt and glycogen synthase kinase 3β rather than autophagy. J. Immunol. *189*, 4154-4164.

Liu, W., Wu, H., Chen, L., Wen, Y., Kong, X., and Gao, W.Q. (2015). Park7 interacts with p47(phox) to direct NADPH oxidase-dependent ROS production and protect against sepsis. Cell Res. *25*, 691-706.

Liu, X., Wu, X.P., Zhu, X.L., Li, T., and Liu, Y. (2017). IRG1 increases MHC class I level in macrophages through STAT-TAP1 axis depending on NADPH oxidase mediated reactive oxygen species. Int. Immunopharmacol. *48*, 76-83.

Mandal, R., Barrón, J.C., Kostova, I., Becker, S., and Strebhardt, K. (2020). Caspase-8: the double-edged sword. Biochim. Biophys. Acta Rev. Cancer *1873*, 188357.

Martinet, W., De Meyer, G.R., Timmermans, J.P., Herman, A.G., and Kockx, M.M. (2006). Macrophages but not smooth muscle cells undergo benzyloxycarbonyl-Val-Ala-DL-Asp(O-Methyl)-fluoromethylketone-induced nonapoptotic cell death depending on receptor-interacting protein 1 expression: implications for the stabilization of macrophage-rich atherosclerotic plaques. J. Pharmacol. Exp. Ther. *317*, 1356-1364.

McComb, S., Cessford, E., Alturki, N.A., Joseph, J., Shutinoski, B., Startek, J.B., Gamero, A.M., Mossman, K.L., and Sad, S. (2014). Type-I interferon signaling through ISGF3 complex is required for sustained Rip3 activation and necroptosis in macrophages. Proc. Natl. Acad. Sci. U. S. A. *111*, E3206-E3213.

Meylan, E., Burns, K., Hofmann, K., Blancheteau, V., Martinon, F., Kelliher, M., and Tschopp, J. (2004). RIP1 is an essential mediator of Toll-like receptor 3-induced NF-kappa B activation. Nat. Immunol. *5*, 503-507.

Pan, Z.K., Fisher, C., Li, J.D., Jiang, Y., Huang, S., and Chen, L.Y. (2011). Bacterial LPS up-regulated TLR3 expression is critical for antiviral response in human monocytes: evidence for negative regulation by CYLD. Int. Immunol. *23*, 357-364.

Pasparakis, M. and Vandenabeele, P. (2015). Necroptosis and its role in inflammation. Nature *517*, 311-320.

Rosenbaum, D.M., Degterev, A., David, J., Rosenbaum, P.S., Roth, S., Grotta, J.C., Cuny, G.D., Yuan, J., and Savitz, S.I. (2010). Necroptosis, a novel form of caspase-independent cell death, contributes to neuronal damage in a retinal ischemia-reperfusion injury model. J. Neurosci. Res. *88*, 1569-1576.

Samie, M., Lim, J., Verschueren, E., Baughman, J.M., Peng, I., Wong, A., Kwon, Y., Senbabaoglu, Y., Hackney, J.A., Keir, M., et al. (2018). Selective autophagy of the adaptor TRIF regulates innate inflammatory signaling. Nat. Immunol. *19*, 246-254.

Schmalz, G., Krifka, S., and Schweikl, H. (2011). Toll-like receptors, LPS, and dental monomers. Adv. Dent. Res. *23*, 302-306.

Seya, T., Shime, H., Takaki, H., Azuma, M., Oshiumi, H., and Matsumoto, M. (2012). TLR3/TICAM-1 signaling in tumor cell RIP3-dependent necroptosis. Oncoimmunology *1*, 917-923.

Shi, C.S. and Kehrl, J.H. (2008). MyD88 and Trif target Beclin 1 to trigger autophagy in macrophages. J. Biol. Chem. *283*, 33175-33182.

Takeda, K., Kaisho, T., and Akira, S. (2003). Toll-like receptors. Annu. Rev. Immunol. *21*, 335-376.

Takemura, R., Takaki, H., Okada, S., Shime, H., Akazawa, T., Oshiumi, H., Matsumoto, M., Teshima, T., and Seya, T. (2015). PolyI:C-induced, TLR3/RIP3-dependent necroptosis backs up immune effector-mediated tumor elimination in vivo. Cancer Immunol. Res. *3*, 902-914.

Vandenabeele, P., Declercq, W., Van Herreweghe, F., and Vanden Berghe, T. (2010b). The role of the kinases RIP1 and RIP3 in TNF-induced necrosis. Sci. Signal. *3*, re4.

Vandenabeele, P., Galluzzi, L., Vanden Berghe, T., and Kroemer, G. (2010a). Molecular mechanisms of necroptosis: an ordered cellular explosion. Nat. Rev. Mol. Cell Biol. *11*, 700-714.

Wang, J., Whiteman, M.W., Lian, H., Wang, G., Singh, A., Huang, D., and Denmark, T. (2009). A non-canonical MEK/ERK signaling pathway regulates autophagy via regulating Beclin 1. J. Biol. Chem. *284*, 21412-21424.

Witt, A. and Vucic, D. (2017). Diverse ubiquitin linkages regulate RIP kinases-mediated inflammatory and cell death signaling. Cell Death Differ. *24*, 1160-1171.

Wu, Y.T., Tan, H.L., Huang, Q., Sun, X.J., Zhu, X., and Shen, H.M. (2011). zVAD-induced necroptosis in L929 cells depends on autocrine production of TNFα mediated by the PKC-MAPKs-AP-1 pathway. Cell Death Differ. *18*, 26-37.

Wu, Y.T., Tan, H.L., Shui, G., Bauvy, C., Huang, Q., Wenk, M.R., Ong, C.N., Codogno, P., and Shen, H.M. (2010). Dual role of 3-methyladenine in modulation of autophagy via different temporal patterns of inhibition on class I and III phosphoinositide 3-kinase. J. Biol. Chem. *285*, 10850-10861.

Xia, X., Lei, L., Wang, S., Hu, J., and Zhang, G. (2020). Necroptosis and its role in infectious diseases. Apoptosis *25*, 169-178.

Xu, Y., Jagannath, C., Liu, X.D., Sharafkhaneh, A., Kolodziejska, K.E., and Eissa, N.T. (2007). Toll-like receptor 4 is a sensor for autophagy associated with innate immunity. Immunity *27*, 135-144.

Xu, Y., Kim, S.O., Li, Y., and Han, J. (2006). Autophagy contributes to caspase-independent macrophage cell death. J. Biol. Chem. *281*, 19179-19187.

Yuan, J., Amin, P., and Ofengeim, D. (2019). Necroptosis and RIPK1-mediated neuroinflammation in CNS diseases. Nat. Rev. Neurosci. *20*, 19-33.

Zhan, Z., Xie, X., Cao, H., Zhou, X., Zhang, X.D., Fan, H., and Liu, Z. (2014). Autophagy facilitates TLR4- and TLR3-triggered migration and invasion of lung cancer cells through the promotion of TRAF6 ubiquitination. Autophagy *10*, 257-268.

Zhang, X., Matsuda, M., Yaegashi, N., Nabe, T., and Kitatani, K. (2020). Regulation of necroptosis by phospholipids and sphingolipids. Cells *9*, 627.

Zheng, M. and Kanneganti, T.D. (2020). The regulation of the ZBP1-NLRP3 inflammasome and its implications in pyroptosis, apoptosis, and necroptosis (PANoptosis). Immunol. Rev. *297*, 26-38.